Available online at www.sciencedirect.com
SCIENCE DIRECT
Polymer 46 (2005) 2381–2388
polymer
www.elsevier.com/locate/polymer

Real-time dynamic light scattering on gelation and vitrification

Mitsuhiro Shibayama[a,*], Satoshi Ozeki[b], Tomohisa Norisuye[b]

[a]Neutron Science Laboratory, Institute for Solid State Physics, University of Tokyo, 106-1 Shirakata, Tokai, Ibaraki 319-1106, Japan
[b]Department of Polymer Science and Engineering, Kyoto Institute of Technology, Matsugasaki, Sakyo-ku, Kyoto 606-8585, Japan

Received 22 August 2004; received in revised form 5 December 2004
Available online 28 January 2005

Abstract

The time-resolved dynamic light scattering has been employed to investigate gelation of divinylbenzene (DVB; branched chains) and vitrification of styrene (St; linear chains) during radical polymerization in bulk. The intensity correlation function (ICF) was obtained every 30 s during polymerization process. The DVB system exhibited a power law behavior in ICF characteristic of gelation threshold, which was followed by vitrification. In the case of St, two relaxation modes appeared before vitrification, which were assigned to be the cooperative and the slow relaxation modes.

Keywords: Vitrification; Gelation; Dynamic light scattering

1. Introduction

Gelation and vitrification are intriguing issues in polymer physics, which involve divergence of connectivity and freezing-in of dynamics, respectively. In the case of the former, chain connectivity diverges at the gelation point and polymer chains are topologically frozen-in [1,2]. However, local chain motion is still allowed even after the gelation point. On the other hand, vitrification means a freezing-in process of the dynamics and is mainly attained by lowering temperature or an increase in the population of the glass forming particles. Vitrification is also observed by increasing cross-linking density in a polymer network as is the case of high density vulcanization of natural rubber to form one of the oldest plastics, i.e. ebonite. Note that rubber contains about 3% of surfer, while ebonite does 30%. In this work, we discuss the difference in polymer chain dynamics during gelation and vitrification by dynamic light scattering.

Virification, i.e. glass formation, has long been one of the central issues of soft condensed matter physics because of it complexity and scientific interests on glass transition [3]. In many cases, glass transition is discussed with respect to temperature. Here, on the other hand, we introduce a system undergoing vitrification with polymerization time for comparison between gelation and vitrification. The glass transition has been investigated by various techniques, such as viscoelasticity [4], dielectrics, and thermal properties. A pioneering work on the competition and vitrification was carried out by Enns and Gillham, who proposed a time-temperature-transformation (TTT) cure diagram for isothermal curing process of an amine-cured epoxy resin [5]. They predicted an 'S'-shape TTT curve diagram and verified it by dynamical mechanical measurements. However, to our knowledge, it is quite few to discuss glass transition from the viewpoint of chain connectivity.

It is now well known that the dynamics of a gel-forming liquid at the gelation threshold is characterized by a power-law behavior in the intensity correlation function (ICF). Such a power law in ICF was observed in synthetic gels [6,7] as well as in natural gels [8,9]. This is due to a formation of self-similar clusters whose longest relaxation time diverges at the gelation threshold [10]. On the other hand, ICFs for sols are well fitted with a stretched exponential function [6,8,11]. As a matter of fact, a clear crossover from a stretched exponential to a power law behavior has been often observed at the gelation threshold [6,9]. Since this power law behavior at the gelation threshold is

* Corresponding author. Tel.: +81 29 287 8904; fax: +81 4 7134 6069.
E-mail address: sibayama@issp.u-tokyo.ac.jp (M. Shibayama).

0032-3861/$ - see front matter © 2005 Elsevier Ltd. All rights reserved.
doi:10.1016/j.polymer.2005.01.018

phenomenologically similar to the β relaxation in glasses as predicted by Göetze [12], the analogy of the sol-gel transition of gelatin gels to the α-to-β transitions in glasses was discussed by Ren and Sorensen [13] and by Ikkai and Shibayama [14]. However, the dynamics of gel forming liquid has not been fully elucidated yet because of the following questions remain unsolved. First, the behavior after the gelation threshold, e.g. $t > t_{th}$, is different dependent on systems, where t and t_{th} are the polymerization time and the time at gelation threshold, respectively. For example, in the case of silica gels made with a basic catalyst [6] and for gelatin gels [8], the power law behavior is preserved for $t > t_{th}$. On the other hand, such a power-law behavior was exclusively observed only at $t \approx t_{th}$ in silica gels prepared with an acidic catalyst [7] and in poly(*N*-isopropylacrylamide) (NIPA) aqueous gels [15]. Particularly, in the case of NIPA gels, the ICF for $t \gg t_{th}$ (or $C \gg C_{th}$) was reduced to a single exponential function assigned to the so-called gel mode, where C and C_{th} are the monomer concentration at preparation and its lowest value necessary for gel formation, respectively [16] Second, the physical meaning and the behavior of the power-law exponent, n, is still controversial. Ren et al. reported that the value of n is dependent on the scattering vector, q. However, none of our systems [7,14,15] exhibited such a q-dependence in n.

The recovery of the stretched exponential or single exponential behavior after gelation threshold may be explained as follows. At the gelation threshold, a divergence of connectivity takes place. After connectivity divergence, only local motions similar to those in semi-dilute polymer solutions are allowed (the so-called gel mode). However, if the temperature is low enough or the cross-link density is high enough to freeze the local motion, even such local motions are forbidden and vitrification takes place instead.

Here, we deal with more idealistic systems to answer the above questions, i.e. bulk polymerization of styrene (St) and divinylbenzene (DVB). Both are one-component systems, but differ in their potential connectivity. St monomers are allowed only linear extension, i.e. formation of linear polymer chains. The glass transition temperature (T_g) of polystyrene(PSt) is around 100 °C. Hence, vitrification may be observed during polymerization if the polymerization is carried out at a temperature below 100 °C. In the case of DVB, on the other hand, each monomer is capable of branching. This leads to a highly branched polymers, and consequently a network structure is formed as discussed by Flory [17]. Therefore, gelation as well as vitrification is expected during polymerization of DVB [18]. In this paper, we try (1) to clarify the difference in the dynamics of polymer chains in the course of vitrification and gelation by time-resolved dynamic light scattering (TRDLS), (2) to propose a relevant method to determine and/or to discriminate the vitrification and gelation, and (3) to discuss the dynamics of post-gelation-threshold.

2. Theoretical section

The time-intensity correlation functions (ICFs), $g^{(2)}(\tau)$, is defined by

$$g^{(2)}(\tau) = \frac{\langle I(\tau_0) I(\tau_0 + \tau)\rangle_T}{\langle I(\tau_0)\rangle_T^2} \tag{1}$$

where $I(\tau_0)$ and $I(\tau_0+\tau)$ indicate the scattered intensities at time τ_0 and at $\tau_0+\tau$, respectively. The subscript T denotes time averaging. In the case of complex fluids, such as gels, the intensity correlation function, $g^{(2)}(\tau)$-1, can be often given by the square of the sum of two terms representing fast and slow modes as follows [6,8,19,20],

$$g^{(2)}(\tau) - 1 = \sigma_I^2 \{A \exp(-\tau/\tau_f) + (1 - A)\exp[-(\tau/\tau_s)^\beta]\}^2 \tag{2}$$

where σ_I^2 is the initial amplitude of ICF, τ_f and τ_s are the characteristic relaxation times of the fast and slow modes, respectively, and A $(0 \le A \le 1)$ is the fraction of the fast mode. The fast mode is the cooperative diffusion of chain molecules [21] 0n the other hand, the slow mode corresponds to the translational diffusion of clusters.

At the gelation threshold, τ_s diverges and a power-law mode appears, which is characterized by the following function,

$$g^{(2)}(\tau) - 1 = \sigma_I^2 \{A \exp(-\tau/\tau_f) + (1 - A)[1 + (\tau/\tau^*)]^{(n-1)/2}\}^2 \tag{3}$$

where τ^* is the lower cut-off of the power-law behavior and n is the critical exponent for the viscoelasticity [6,22,23]. The power law behavior indicates gelation threshold. This exponent is the same as that obtained by mechanical dispersion [24,25]. Winter reported $n \approx 0.5$ for polydimethylsiloxane and Durand et al. [25] obtained $n \approx 0.73$. Muthukumar explained these variations in n in terms of the degree of screening of excluded volume effect and hydrodynamics [26].

3. Experimental section

3.1. Samples

Reagent grade St monomer was used for the experiment without further purification. Divinylbenzene (DVB) was received from Mitsubishi Chem. Co., Ltd, which contained 19 wt% of ethylvinylbenze. Monomers, i.e. either St or DVB, were mixed with the initiator (2,2′-azobisisobutyronitrile; AIBN, 0.8 wt% unless specified) and stirred for 10 min, followed by filtration with a 0.25 μm-filter. Then, each of the monomer samples was polymerized in a test tube of 10 mm-diameter at 60 °C.

3.2. TRDLS

The TRDLS measurements were carried out on an ALV compact goniometer system, ALV, Langen, Germany, with a 22 mW helium-neon laser source. A strong scattered intensity and a high coherence in ICF (more than 0.98) were obtained owing to an employment of a set of a static and dynamic enhancers and a high-quantum efficient avalanche-photo diode detection system. The sampling time was 30 s and the scattering angle, θ, was 90° unless specified. The samples under polymerization were occasionally quenched by cooling in ice and were used for a flow test and for a more quantitative analysis of ICF.

3.3. Gel permeation chromatography (GPC)

Polystyrene(PSt) precursors are sampled at several stages of polymerization, weighted, precipitated with methanol, and then completely dried. After determining the conversion (i.e. yield) of the polymerization by gravimetry, the molecular weights and polydispersity index of dried PSt's were evaluated with a GPC (Model GPC System-21, Showa Denko, Co. Ltd, Tokyo) at a temperature of 40 °C with chloroform.

4. Results and discussion

4.1. Determination of gelation threshold

Fig. 1 shows time variations of scattered intensity $\langle I\rangle_T$ for (a) St(100%), (b) St/DVB(50%/50%), and (c) DVB(100%). The behavior of $\langle I\rangle_T$ was quite different on the fact whether or not the system is capable of gelation. In the case of St(100%) (capable only of chain extension without branching formation or cross-linking), the variation of $\langle I\rangle_T$ was rather small for $t \approx 10$ h. Then, $\langle I\rangle_T$ started to fluctuate. On the other hand, St/DVB(50%/50%) and DVB(100%), capable of gelation, exhibited a stepwise increase in $\langle I\rangle_T$ at $t < 3.138$ and 4.888 h, respectively, as shown by the vertical lines. After the step-wise increase, $\langle I\rangle_T$ strongly fluctuates with time. This indicates that the system becomes nonergodic [27].

Fig. 2 shows time evolutions of ICFs for (a) St(100%), (b) St/DVB(50%/50%), and (c) DVB(100%). Characteristic features depending on the capability of gelation are also seen in this figure. The ICFs for St(100%) systems show clear two relaxation modes for $t < 7$ h, and then ICF becomes flattened. The ICFs for St/DVB(50%/50%) and DVB(100%) exhibit a power-law behavior exclusively at $t = t_{th} = 3.138$ h (St/DVB(50%/50%)), and $t = t_{th} = 4.888$ h (DVB(100%)) before flattening takes place. Therefore, it is clear from Figs. 1 and 2 that gelation takes place $t = t_{th}$ in the systems of St/DVB(50%/50%) and DVB(100%) and the gelation threshold can be clearly resolved by TRDLS as a power-law behavior in ICF.

It is known that glasses and gels are nonergodic media [27]. The nonergodicity is observed as strong fluctuations in the scattered intensity, resulting in a depression of σ_I^2. The vitrification and gelation, therefore, should be observed by TRDLS. Fig. 3 shows the variations of the initial amplitude of ICF, σ_I^2, as well as $\langle I\rangle_T$ as a function of polymerization time, t, for (a) St(100%) and (b) DVB(100%). In the case of St(100%), a depression of σ_I^2 is observed at $t \approx 9.667$ h (the arrow), and concurrently $\langle I\rangle_T$ starts to fluctuate. This may be the time at which the St system undergoes vitrification. However, this statement will be examined later. σ_I^2 for DVB(100%) starts to decrease at 4.888 h (the arrow). The times are in accordance with those for the stepwise increase in $\langle I\rangle_T$. In our previous paper, we proposed four methods to determine gelation threshold [7]; (1) an abrupt increase in $\langle I\rangle_T$, (2) an appearance of power law behavior in ICF, (3) a characteristic broadening in the decay time distribution function, and (4) a depression of σ_I^2. It is needless to mention that the results in Figs. 1–3 correspond to (1), (2), and (4), respectively. Hence, it is clear that the gelation threshold can be determined by TRDLS.

Fig. 4(a) shows the comonomer concentration

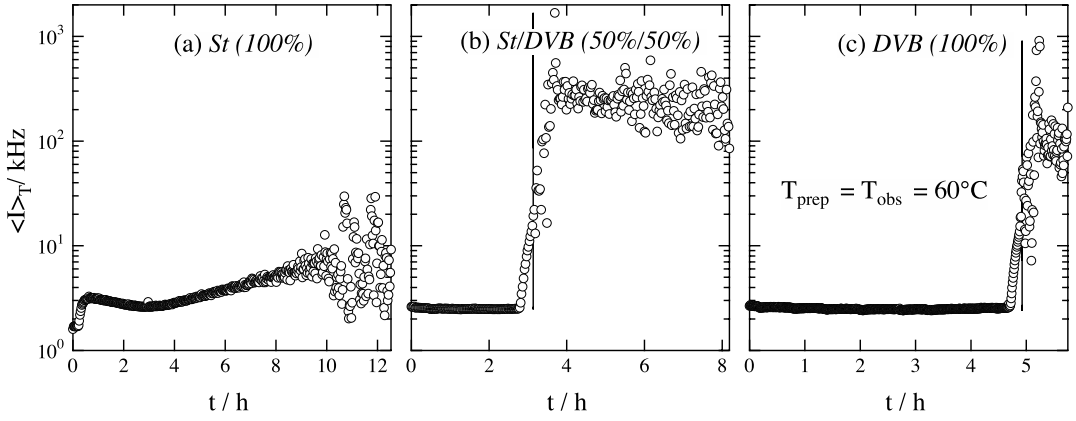

Fig. 1. Variation of the scattered intensity, $\langle I\rangle_T$, for (a) St(100%), (b) St/DVB(50%/50%), and (c) DVB(100%) as a function of polymerization time, t. The vertical lines indicate the time at gelation threshold.

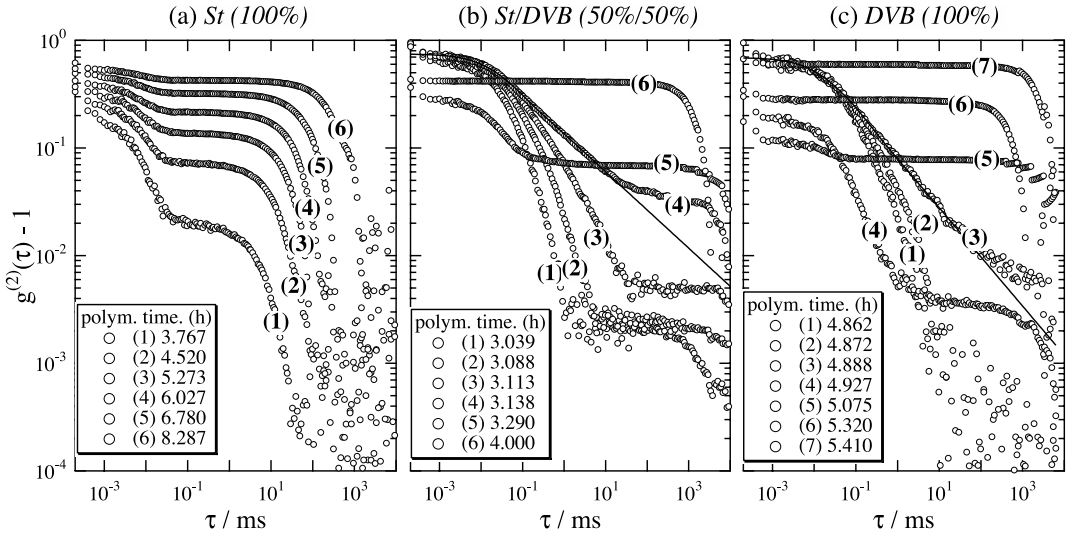

Fig. 2. Comparison of the time-intensity correlation functions (ICF) during polymerization process for (a) St(100%), (b) St/DVB(50%/50%), and (c) DVB(100%). The solid lines indicate fits with a power law function (Eq. (2)).

dependence of t_{th}, where $C_{Styrene}$ is the concentration of styrene monomer. The polymerization temperature was 60 °C. It should be noted that t_{th} is a decreasing function of $C_{Styrene}$. An increase of $C_{Styrene}$ means that a decrease of cross-linker concentration C_{DVB}. Hence, it was naively expected that the higher the $C_{Styrene}$, the slower the rate of gelation. This unexpected result can be interpreted as follows. A styrene monomer plays as a chain extender so that a propagating chain with a higher $C_{Styrene}$ can reach to another chain for cross-linking faster than with a lower $C_{Styrene}$. If there are no St monomers in the reactor batch, DVB momomers form densely packed aggregates. It would take longer time to fill the space necessary for gelation than a system containing St monomers. Fig. 4(b) and (c) shows the result of (b) preparation temperature, T_{prep}, dependence and (c) initiator concentration, C_{AIBN}, dependence for St/DVB(50%/50%). These results were quite reasonable as a radical polymerization of vinyl monomers.

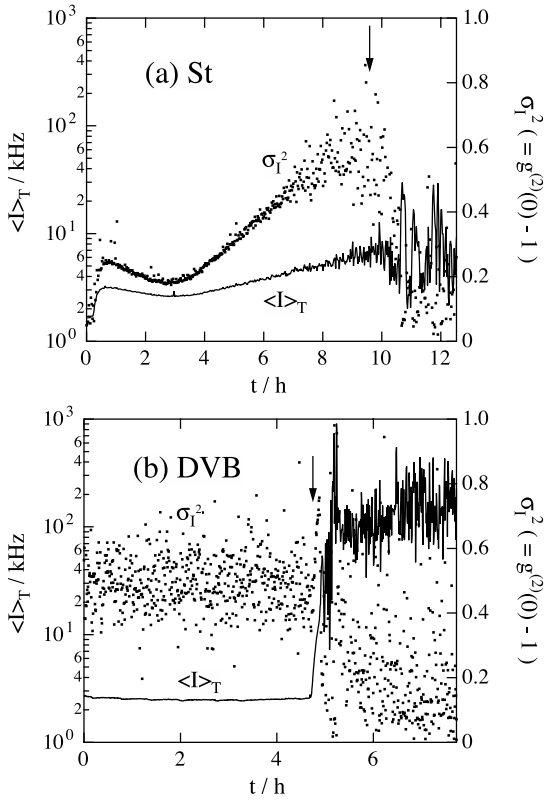

Fig. 3. Polymerization time dependence of $\langle I \rangle_T$ and the initial amplitude of ICF, σ_I^2, for (a) St(100%) and (b) DVB(100%) systems. The arrows indicate (a) the time at nonergodicity appears and (b) the gelation threshold.

4.2. Analysis of gelation

Fig. 5 shows the time evolution of ICFs near the gelation threshold for DVB. The solid lines are obtained by fitting with Eqs. (2) (solid lines) and (3) (dashed line). The fitting with Eq. (2) indicates that the slow mode seems to be similar to the α-relaxation as observed in glass forming materials above the glass transition temperature [28]. A power-law behavior, on the other hand, appears exclusively at $t =$ 4.888 h (the dashed line; curve 3). Note that ICF curves numbered (3)–(5) were sequentially obtained with the duration of 30 s. Therefore, the time-resolution for detecting a power-law behavior, in another word, the time-resolution of the gelation threshold, by TRDLS, is in the order of 10 s.

The value of n for DVB was $n \approx 0.50$, irrespective of q ($30° < \theta < 150°$). A similar value for $n(\approx 0.4)$ was reported for polyvinyl alcohol–Congo Red and NIPA gels [15], which are also q independent. These results disagree to the result reported by Ren and Sorensen [8,13]. The q-independence of the power law exponent indicates that the system at the gelation threshold is a fractal object and does not have a characteristic scale length [10]. After the gelation threshold

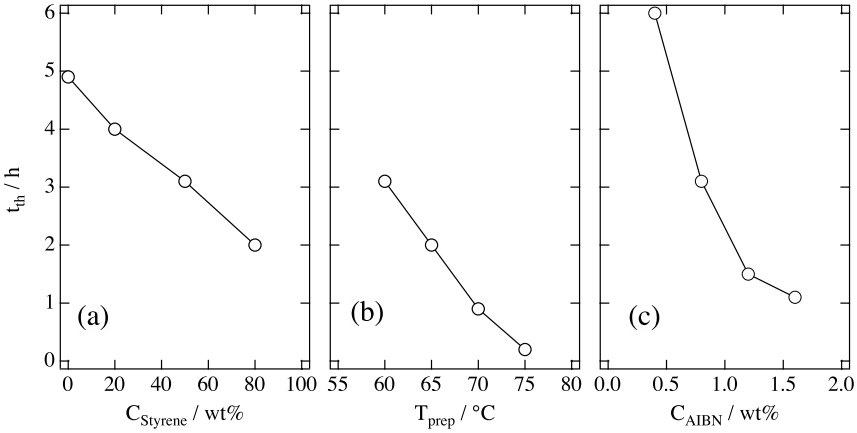

Fig. 4. Styrene monomer concentration, $C_{styrene}$, (b) polymerization temperature, and (c) initiator concentration, C_{AIBN}, dependence of the time at gelation threshold.

($t=4.888$ h), the ICF becomes to have the fast and slow modes (curve (4) in Fig. 5). For $t>5.410$ h, ICF did not change noticeably with t. It should be noted that a drastic change in flow behavior was observed between curve (6) (viscous) and curve (7) (glassy). Therefore, it is concluded that vitrification took place between $t=5.320$ h and $t=5.410$ h.

The variation of n with $C_{Styrene}$ is plotted in Fig. 6. According to the prediction, n was expected to decrease with $C_{Styrene}$ because the degree of branching decreases with $C_{Styrene}$. According to Muthukumar [26], the value of n can vary from 0 to 1, depending on the degrees of screening of hydrodynamic and excluded volume interactions, as given by

$$n = \frac{d(d+2-2d_f)}{2(d+2-d_f)} \tag{4}$$

where d and d_f are the space and fractal dimensions, respectively. However, the observed n did not increase with lowering $C_{Styrene}$ and had a maximum around $C_{Styrene} \approx 0.4$. As a matter of fact, the value of n itself scatters considerably (e.g. ± 0.2). This is partially due to nonergodic nature of gels. Therefore, we give up a further discussion on the $C_{Styrene}$ dependence of n at this stage.

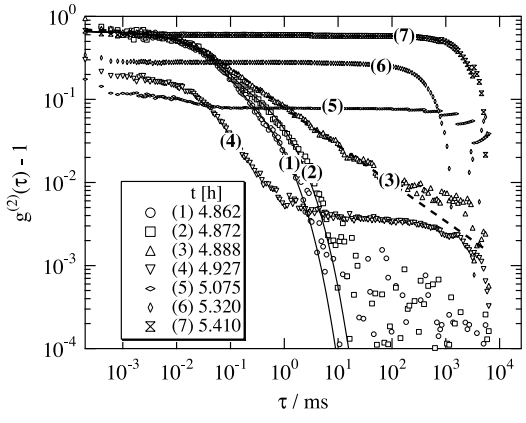

Fig. 5. Time evolution of the intensity correlation functions (ICFs) near the gelation threshold for DVB during bulk polymerization at 60 °C. The solid lines and the dashed line are the fits with Eqs. (1) and (2), respectively.

4.3. Analysis of vitrification

Fig. 7 shows the time evolution of ICFs for St obtained at $\theta=90°$. As indicated by the solid lines, the ICFs were successfully fitted with a combined function of a single and stretched exponential functions given by Eq. (2). Note that no power-law behavior was observed in this case. The fast mode may correspond to the cooperative diffusion mode as often observed in polymer gels and in semi-dilute polymer solutions. The slow mode, on the other hand, may be assigned to the large-scale heterogeneities as observed by Heckmeier et al. in concentrated PSt solutions in toluene [29]. They observed large-scale inhomogeneities of the order of a few hundred angstroms by both static light scattering and dynamic light scattering, which increased with lowering temperature and increasing polymer concentration. These speculations, i.e. the presence of large scale inhomogeneities, were supported by examining the q dependence of the individual modes.

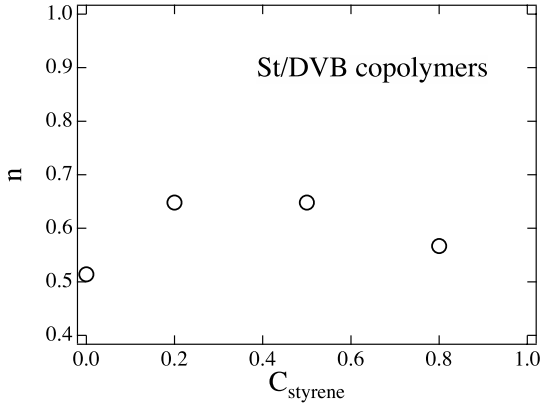

Fig. 6. $C_{styrene}$ dependence of the power-law exponent, n.

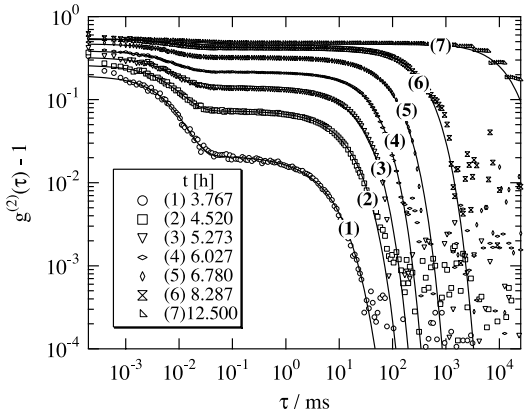

Fig. 7. Time evolution of the intensity correlation functions (ICFs) for St during bulk polymerization at 60 °C. The solid lines are the fits with Eq. (1).

It is crucial to examine q dependence of the characteristic decay rates for the fast and slow modes, τ_f^{-1} and τ_s^{-1}. Fig. 8(a) shows the q dependence of τ_f^{-1} and τ_s^{-1} at $t=3.767$ h (curve 1) for the scattering angle of $30° \leq \theta \leq 150°$. The results indicate $\tau_f^{-1} \sim q^{-2}$ and $\tau_s^{-1} \sim q^{-2}$. This result is in good agreement with those reported by Heckmeier for PSt ($M_w = 7.8\times10^4$, $M_w/M_n = 1.02$) in toluene (12.5–25%) [29]. However, as shown in Fig. 8(b), both τ_f^{-1} and τ_s^{-1} deviate from a q^2-dependent behavior to $\tau_f^{-1} \sim q^{3.32}$ and $\tau_s^{-1} \sim q^{2.46}$ at $t=6.780$ h (curve 5). These results indicate that both fast and slow modes are diffusive at least $t \leq 3.767$ h, but become non-diffusive with t.

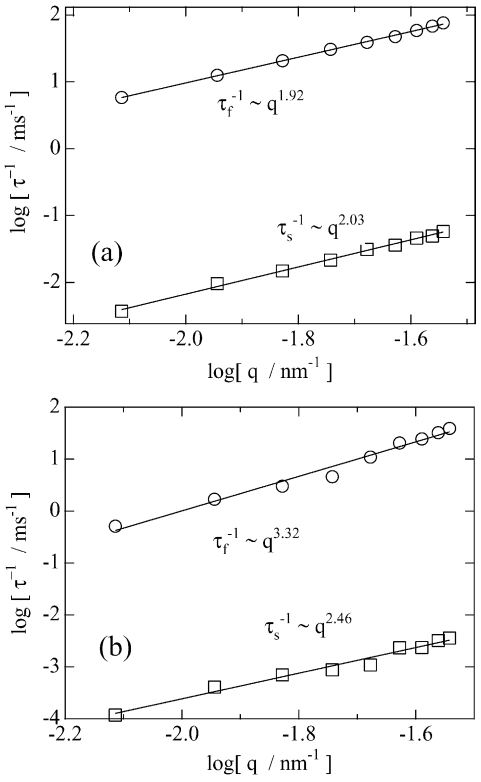

Fig. 8. q dependence of the characteristic relaxation times, τ_f and τ_s at (a) the early ($t=3.767$ h) and (b) the late stage ($t=6.780$ h).

Fig. 9 shows the variations of A, β, τ_f, and τ_s as a function of polymerization time t. The data are highly scattered at the beginning of polymerization, i.e. for $t < 3$ h. This is because that the polymer chains do not grow well at this stage. For $t > 3$ h, τ_f is rather invariant, while A is a monotonous decreasing function of t. The cooperative diffusion coefficient D ($\approx 1/q^2\tau_f$) is estimated to be 2×10^{-6} cm^2/s, which is rather close to that of typical polymer gels, such as NIPA gels and the corresponding solutions, e.g. 5×10^{-7} cm^2/s [16]. Therefore, it can be conjectured that the fast mode at the early stage is assigned to be a gel mode due to entangled network chains as often observed in semi-dilute polymer solutions. The variation of τ_f and A indicates that further polymerization simply results in a decrease in the fraction of the fast mode, A, without loosing local mobility, D. The slow mode also exhibits a characteristic feature for $3 < t < 10$ h. That is, the value of τ_s increases exponentially with t, while β stays near unity for $3 < t < 10$ h.

In order to assign the slow mode, the conversion and the molecular weights of polystyrene precursors were characterized by GPC. Fig. 10 shows (a) conversion, (b) the number, M_n, and weight average molecular weights, M_w, and (c) the polydispersity index, M_w/M_n. It should be noted here that M_w/M_n remains to be around 2 (as indicated with the dashed line). Since $M_w/M_n \approx 2$, it is assured that the system has a most-probable distribution of the molecular weight, which is predicted for radical polymerization. Hence, this result suggests that the polymerization reaction took place such that polymer chains with a characteristic molecular weight, i.e. $M_n \approx 5.0\times10^3$, appear suddenly and the number of the polymer chains increases rather time linearly.

As shown in Fig. 10(a), the conversion increases time-linearly from 40 to 60%. The growth of M_n and M_w, on the other hand, are rather slow. Therefore, the time dependence of the molecular weight cannot be responsible for the exponential growth of τ_s (Fig. 7). Although the slow mode for $t \ll 10$ h definitely correspond to the longest relaxation of polymer chains in concentrated solutions [4,30], its

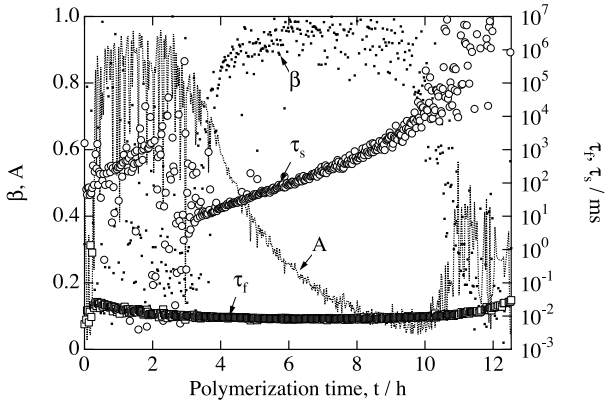

Fig. 9. Polymerization time dependence of the stretched exponent, β, the fraction of the diffusive mode, A, and the characteristic relaxation times, τ_f and τ_s for St.

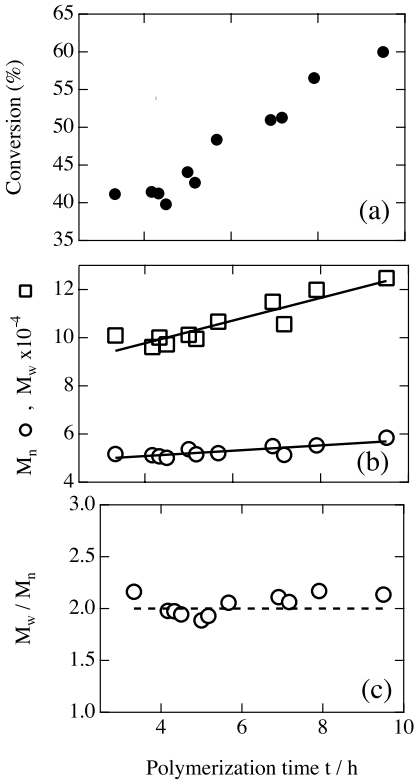

Fig. 10. Polymerization time dependence of (a) conversion, (b) the number M_n and weight average molecular weights, M_w, and (c) the polydispersity index, M_w/M_n.

growth is ascribed not only to the increase of molecular weight but also to that of polymer fraction in the reactor batch. Therefore, it is necessary to incorporate the change of conversion during the polymerization in order to understand the strong polymerization time dependence of τ_s.

Now, we try a semi-qualitative discussion on the polymerization time dependence of τ_s. If τ_s corresponds to the longest relaxation time of polymer chains in a solvent, it scales with the viscosity η and translational diffusion coefficient D_{tr}, as follows;

$$\tau_s \sim \eta \sim 1/D_{tr} \tag{5}$$

For entangled polymer chains, η scales with M,

$$\eta \sim M^{3.4} \tag{6}$$

On the other hand, D_{tr} can be assumed to be a function of polymer concentration, C [31,32],

$$D \sim C^{-2} \quad \text{(Rouse friction, } \Theta \text{ solvent)} \tag{7}$$

$$D \sim C^{-3} \quad \text{(Stokes friction, } \Theta \text{ solvent)} \tag{8}$$

In the case of PSt polymerized from St monomers without solvent, its dynamics is expected to be Stokes friction in a Θ solvent. Hence, τ_s can be reduced to $\tau_s/C^3M^{3.4}$, which is now C and M invariant. Fig. 11 shows polymerization time dependence of $\tau_s/C^3M^{3.4}$, where we chose $M=M_w$. Different from our expectation, $\tau_s/C^3M^{3.4}$ is

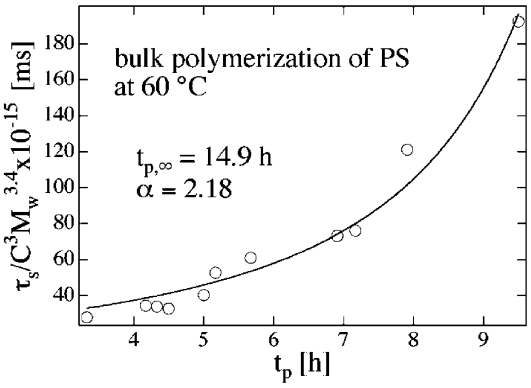

Fig. 11. Polymerization time dependence of the reduced relaxation time, $\tau_s/C^3M^{3.4}$ for the styrene system.

an increasing function of t. One important fact which was not considered in the reduction of τ_s was that the system approaches the glass transition as polymerization goes on since the polymerization temperature is 60 °C (which is significantly lower than that of bulk PSt). If it is correct, τ_s may increase dramatically by polymerization proceeds. The solid line in the figure was obtained by fitting the data with

$$\frac{\tau_s}{C^3M^{3.4}} \sim |t - t_\infty|^{-\alpha} \tag{9}$$

where t_∞ and α are the time and the exponent related to the divergence of the slow mode. This function was employed analogous to the equations appearing in critical phenomena [33]. From this analysis, $t_\infty = 14.9$ h and $\alpha \approx 2.2$ were obtained. The time at which the slow mode diverges may correspond to the glass transition time. Let us examine this conjecture in more detail. The glass transition temperature was evaluated by differential scanning calorimetry (DSC) to be 67 °C for PSt quenched at $t=12.5$ h. Since this temperature is indeed higher than the polymerization temperature, 60 °C, it is confirmed that a vitrification took place between 8.29 (curve 6 in Fig. 7) $< t <$ 12.5 h (curve 8). Although the prediction with Eq. (9) gives a larger value of glass transition time, the analysis shown above gives a rough estimate of the glass transition time.

At the end of discussion, it should be mentioned that the systems capable of gelation, DVB/PSt, also end up by vitrification as polymerization proceeds. This is why the curve 7 in Fig. 5 and curve 7 in Fig. 7 are indistinguishable. A more quantitative analysis on gelation and vitrification is in progress.

5. Conclusion

The dynamics of linear and branched chain molecules was studied by time-resolved dynamic light scattering during their polymerization processes. It was found that the polymerization of St monomers exhibits two relaxation modes, i.e. the cooperative diffusion and the longest

relaxation of polymer chains in concentrated solutions. The latter changes to the so-called α-relaxation mode at the late stage of polymerization. As the polymerization proceeds, the fraction of the cooperative diffusion mode diminishes. Finally, the system reaches the point at which nonergodicity appears characterized by vigorous fluctuations in $\langle I \rangle_T$ and depression of σ_I^2, which is followed by vitrification. On the other hand, the systems capable of cross-linking showed a distinct gelation threshold, characterized by a power-law behavior in ICF and the appearance of nonergodicity. Hence, it is disclosed here that gelation and vitrification can be clearly distinguished by TRDLS. In the case of the systems containing DVB, the gelation is followed by vitrification and the dynamics becomes similar to that of linear chains at the late stage of polymerization.

Acknowledgements

The authors are grateful to T. Kanaya, Institute for Chemical Research, Kyoto U., Y. Shiwa and Y. Tsukahara, Kyoto Inst. of Tech. for valuable discussions. This work is partially supported by the Ministry of Education, Science, Sports and Culture, Japan (Grant-in-Aid, 09450362 and 10875199 to M.S.). Thanks are due to the Cosmetology Research Foundation, Tokyo, for financial assistance.

References

[1] Guenet JM. Thermoreversible gelation of polymers and biopolymers. New York: Academic Press; 1992.
[2] Shibayama M, Norisuye T. Bull Chem Soc Jpn 2002;75:641.
[3] Donth E. The glass transition. Berlin: Springer; 2001.
[4] Ferry JD. Viscoelastic properties of polymers. 3rd ed. New York: Wiley; 1980.
[5] Enns JB, Gillham LK. J Appl Polym Sci 1983;28:2567.
[6] Martin JE, Wilcoxon J. Phys Rev Lett 1988;61:373.
[7] Norisuye T, Shibayama M, Tamaki R, Chujo Y. Macromolecules 1999;32:1528.
[8] Ren SZ, Shi WF, Zhang WB, Sorensen CM. Phys Rev A 1992;45: 2416.
[9] Lang P, Burchard W. Macromolecules 1991;24:814.
[10] Stauffer D. Introduction to percolation theory. London: Taylor and Francis; 1985.
[11] Adam M, Delsanti M, Munch JP, Durand D. Phys Rev Lett 1988;61: 706.
[12] Goetze W, Sjogren L. Prog Rep Phys 1992;55:241.
[13] Ren SZ, Sorensen CM. Phys Rev Lett 1993;70:1727.
[14] Ikkai F, Shibayama M. Phys Rev Lett 1999;82:4946.
[15] Takeda M, Norisuye T, Shibayama M. Macromolecules 2000;33: 2909.
[16] Norisuye T, Takeda M, Shibayama M. Macromolecules 1998;31: 5316.
[17] Flory PJ. Principles in polymer chemistry. Ithaca: Cornell University; 1953.
[18] Shibayama M, Ozeki S, Norisuye T. AIP Conf Proc 2000;519:158.
[19] Nystrom B, Roots J, Carlsson A, Lindman B. Polymer 1992;33:2875.
[20] Martin JE, Wilcoxon J, Odinek J. Phys Rev A 1991;43:858.
[21] Tanaka T, Hocker LO, Benedek GB. J Chem Phys 1973;59:5151.
[22] Onuki A. Non-Cryst Solids 1994;172–174:1151.
[23] Adam M, Lairez D. In: Cohen Addad JP, editor. Physical properties of polymeric gels. New York: Wiley; 1996. p. 87.
[24] Winter HH, Chambon F. J Rheology 1986;30:367.
[25] Durand D, Delsanti M, Adam M, Luck JM. Europhys Lett 1987;3:297.
[26] Muthukumar M. Macromolecules 1989;22:4656.
[27] Pusey PN, van Megen W. Physica A 1989;157:705.
[28] Mezei F, Knaak W, Farago B. Phys Rev Lett 1987;58:571.
[29] Heckmeier M, Mix M, Strobl G. Macromolecules 1997;30:4454.
[30] Bird RB, Armstrong RC, Hassager O. Dynamics of polymer liquids. New York: Wiley; 1987.
[31] de Gennes PG. Macromolecules 1986;19:1245.
[32] Pajevic S, Bansil R, Konak C. Macromolecules 1995;28:7536.
[33] Stanley HE. Introduction to phase transition and critical phenomena. New York: Oxford University Press; 1971.